Proceedings of ICFTBA 2026 Symposium: Digital Government, Finance, Accountability, and Sustainable Economic Development
DOI: 10.54254/2754-1169/2026.AB39173

A Two-Stage SARIMA–GARCH Approach to Forecasting Global Monthly Carbon Dioxide Emissions: Trend, Seasonality, and Mitigation Implications

Jingyi Guo

School of Mathematics and Physics, Xi'an Jiaotong-Liverpool University, Suzhou, China
Jingyi.Guo24@student.xjtlu.edu.cn

Abstract. Accurate near-term projections of carbon dioxide (CO_2) emissions help governments gauge progress toward the Paris temperature goals and time demand-side mitigation. Most forecasts rely on annual figures, overlook the pronounced within-year movement of emissions and their reaction to sudden shocks, and rarely model the resulting volatility. Using the IEA–EDGAR v8.0 global monthly fossil CO_2 inventory (156 observations, January 2010–December 2022), this study builds a two-stage model: a seasonal autoregressive integrated moving-average (SARIMA) mean equation selected by an exhaustive search, followed by a GARCH(1,1) variance equation when an ARCH-LM test detects heteroskedasticity. STL decomposition shows a mild upward trend with a strong annual cycle—the seasonal component accounts for 73.9% of short-term fluctuation, with December–January peaks and August–September troughs. The selected mean model is SARIMA(1,0,0)(1,1,1)12 with drift (Ljung–Box p = 0.96), and the GARCH(1,1) removes the remaining ARCH effect (p = 0.27). With MAPE of 1.01% in sample and 2.55% in a held-out 2022 test set and Theil's U of 0.76, it projects 38.86 Gt in 2023 and 39.00 Gt in 2024, a rise of only 0.38% consistent with the Global Carbon Budget's near-plateau. A plateau is far from the rapid, sustained cuts needed for 1.5 °C, so the paper closes with season- and sector-targeted mitigation measures.

Keywords: Global CO_2 emissions, SARIMA, GARCH, seasonal time series, emission forecasting

1. Introduction

Carbon dioxide (CO_2) generated by fossil fuel combustion and industrial processes represents the single largest anthropogenic driver of atmospheric radiative forcing. Although land-use change is another key source of anthropogenic CO_2 emissions, this study centers on fossil-fuel and industrial CO_2 emissions to match the coverage of global high-frequency emission datasets. To stabilise the global climate, anthropogenic greenhouse gas emissions must reach their peak and follow a steep decline trajectory. The Paris Agreement commits signatory countries to holding global warming well below 2 °C above pre-industrial levels and pursuing efforts to limit warming to 1.5 °C [1]. These

© 2026 The Authors. This is an open access article distributed under the terms of the Creative Commons Attribution License 4.0 (https://creativecommons.org/licenses/by/4.0/).

DOI: 10.54254/2754-1169/2026.AB39173

temperature targets demand credible, frequently updated emission baselines to track progress toward climate goals [2].

Annual emission inventories, which are often released several months after the reference year, are too coarse and time-lagged to support timely climate governance. Global CO_2 emissions vary markedly within a single year, responding rapidly to changes in energy demand, weather conditions and economic shocks. The 2020 COVID-19 pandemic vividly exposed this limitation: daily global emissions fell by roughly 17% at the height of lockdown measures, only to rebound within months as containment policies were relaxed [3].

A monthly emission forecasting framework is therefore of great practical value and research necessity. In addition to compensating for the publication lag of annual inventories, such a framework can capture the seasonal emission fluctuations driven by heating and cooling energy demand, detect early deviations from the expected emission path, and quantify uncertainty through prediction intervals rather than single point estimates. The resulting baseline can serve multiple purposes: supporting near-term climate target tracking, identifying abnormal emission shocks, and providing a reference for scenario analysis of emission trends.

Although abundant research has been conducted on emission forecasting, three key research gaps remain. First, most existing studies focus on annual national-level emission totals. The low temporal resolution of annual data fails to capture within-year seasonal patterns and the rapid dynamics of abrupt emission shocks, while the sub-national seasonal time-series research that does exist is mostly limited to individual cities or monitoring stations. Second, prevailing machine learning-based forecasting approaches often prioritise prediction accuracy over model interpretability. These methods typically require large samples with rich feature variables, and few have systematically examined the time-varying volatility of emission residuals. Third, there is still a scarcity of truly global monthly emission studies that integrate seasonal decomposition, rigorous out-of-sample validation, volatility modelling, and practical policy relevance in a unified analytical framework.

Against this backdrop, the characteristic seasonal cycle and crisis-induced uncertainty of global CO_2 emissions remain under-explored, which constitutes the core research gap this study aims to address.

To fill the above gap, this study characterises the long-term trend and annual seasonal pattern of global monthly fossil-fuel and industrial CO_2 emissions. A SARIMA model is constructed and evaluated to characterize the mean process of emissions, while a GARCH model is employed to capture time-varying volatility. The SARIMA model is validated using data from 2022 as a holdout sample and subsequently used to generate 24-month emission forecasts with 95% prediction intervals. The corresponding implications for climate-change mitigation are then discussed based on the empirical findings.

The remainder of this paper is organised as follows. First, existing research on global CO_2 emission trends and forecasting methods is reviewed. The model specifications and analytical procedures employed in this study are then introduced, followed by the empirical estimation results and an evaluation of out-of-sample forecasting performance. Finally, the main findings are summarized, policy recommendations are presented, and the study's limitations are discussed.

2. Literature review

2.1. Trends in global CO_2 emissions

Fossil CO_2 emissions from coal, oil and gas combustion and industrial processes do not follow a smooth annual trajectory. Their monthly dynamics are closely tied to energy demand, which is

DOI: 10.54254/2754-1169/2026.AB39173

jointly shaped by macroeconomic activity and seasonal weather cycles. This inherent within-year variability makes monthly and seasonal analysis indispensable for understanding emission drivers, and differentiates high-frequency research from traditional annual accounting studies.

From the perspective of long-term annual trends, data from the Global Carbon Project shows that global fossil CO_2 emissions sustained a prolonged growth throughout the 2010s. After plateauing in 2019, emissions experienced a notable contraction in 2020, before resuming growth in subsequent years. Specifically, global fossil CO_2 emissions fell by 6.3% (2,232 Mt) in 2020 compared to 2019 levels, then rebounded in 2021. Emissions grew by approximately 1.3% in 2023 to reach around 37 Gt, with a provisional growth estimate of only 0.8% for 2024 [4, 5]. The persistence of such shock-induced deviations from the long-term trend is largely influenced by post-crisis fiscal stimulus policies [6].

The COVID-19 pandemic also triggered unprecedented short-term emission fluctuations at the daily level. At the peak of global lockdown measures in early April 2020, daily global CO_2 emissions dropped by about 17% relative to pre-pandemic levels, with surface transport accounting for nearly half of the reduction [3]. This sharp but temporary daily decline further illustrates how rapidly emissions can respond to external shocks, highlighting the limitation of annual data in capturing abrupt changes.

Beyond long-term trends and short-term shocks, global fossil CO_2 emissions exhibit a distinct seasonal cycle. Driven by heating demand in winter and cooling demand in summer, the seasonal pattern is particularly pronounced in the Northern Hemisphere due to its larger land mass and higher population concentration. The magnitude of this regular annual seasonal fluctuation is substantial, which further emphasises the importance of monthly-level analysis for accurate emission monitoring and forecasting.

2.2. Forecasting CO_2 emissions

The Box–Jenkins ARIMA family remains a benchmark because it is transparent, parsimonious and supplies interval forecasts [7]. Seasonal extensions perform well where data repeat annually: an optimised SARIMA reproduced the trend and seasonal variation of atmospheric CO_2 at Bengaluru, and SARIMAX and Holt–Winters ranked among the strongest statistical models for Indian emissions, though a long short-term memory network gave the lowest error [8, 9]. Chinese work points the same way, coupling ARIMA–BP with LSTM to project carbon intensity and fitting ARIMA(2,1,0) for Gansu with MAPE of 1.6% [10, 11]. Recurring weaknesses are annual data, missing hold-out tests and prediction intervals, and—crucially—the lack of conditional heteroskedasticity tests even though crisis shocks cluster in time, which the two-stage application below addresses.

3. Model and methodology

3.1. Two-stage SARIMA–GARCH specification

A SARIMA model extends ARIMA and is denoted SARIMA(p,d,q)(P,D,Q)s, where p, d and q are the non-seasonal autoregressive (AR), differencing and moving-average (MA) orders, P, D and Q their seasonal counterparts, and s is the seasonal period—twelve for monthly data [7]. With B the backshift operator, the general mean equation is

$$\Phi_P(B^s)\,\varphi_p(B)(1-B)^d(1-B^s)^D y_t = c + \Theta_Q(B^s)\,\theta_q(B)\,\varepsilon_t \tag{1}$$

DOI: 10.54254/2754-1169/2026.AB39173

where φ and Φ are non-seasonal and seasonal AR polynomials, θ and Θ the corresponding MA polynomials, c a drift term and ε_t the disturbance. The automated search selects $d = 0$, $D = 1$, one non-seasonal AR and one seasonal AR and MA term, giving:

$$(1 - \varphi_1 B)(1 - \Phi_1 B^{12})(1 - B^{12}) y_t = c + (1 + \Theta_1 B^{12})\, \varepsilon_t \tag{2}$$

namely SARIMA(1,0,0)(1,1,1)12 with drift: seasonal differencing removes the annual unit root and the drift captures average monthly growth. As shocks cluster over time, the second stage models the conditional variance of ε_t with GARCH(1,1):

$$\sigma_t^2 = \omega + \alpha_1\, \varepsilon_{t-1}^2 + \beta_1\, \sigma_{t-1}^2 \tag{3}$$

where σ_t^2 is the conditional variance, ω a constant, α_1 the ARCH coefficient and β_1 the persistence coefficient. The SARIMA mean supplies point and interval forecasts; GARCH absorbs shock-driven heteroskedasticity, and stationarity requires $\alpha_1 + \beta_1 < 1$.

3.2. Data and modelling procedure

The data are the IEA–EDGAR v8.0 monthly CO_2 series, which allocates annual emissions across months using sector-specific temporal profiles [12, 13]. Country values in gigagrams were summed to global totals and divided by 1,000 to obtain million tonnes (Mt), retaining January 2010–December 2022 (156 observations). The series was decomposed with STL using a periodic seasonal window and robust loess [14]. The seasonal contribution is the ratio of the seasonal standard deviation to the series.

Stationarity was tested with the augmented Dickey–Fuller (ADF) test and ACF/PACF correlograms to lag 36. The mean model was selected by an exhaustive auto.arima search minimising the corrected Akaike criterion. Residuals were checked with Ljung–Box (lag 12) and ARCH-LM tests; on a significant result a Gaussian GARCH(1,1) was fitted with rugarch and the residuals retested. Out-of-sample validity used a 2010–2021 fit, twelve-month 2022 forecasts with 95% intervals and standard accuracy metrics, after which the model was refitted to project 2023–2024 [15].

4. Empirical analysis and results

4.1. Exploratory analysis and decomposition

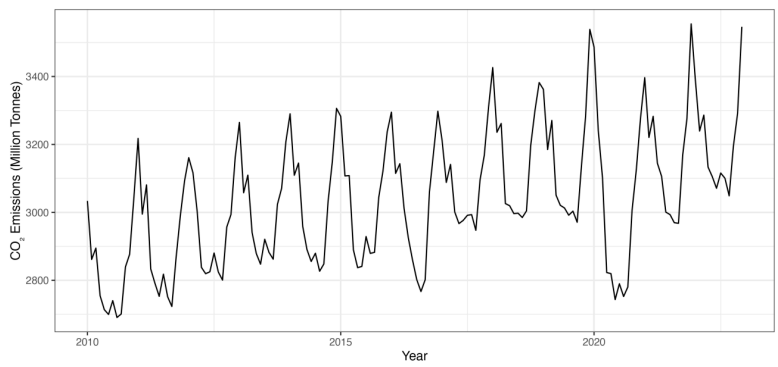
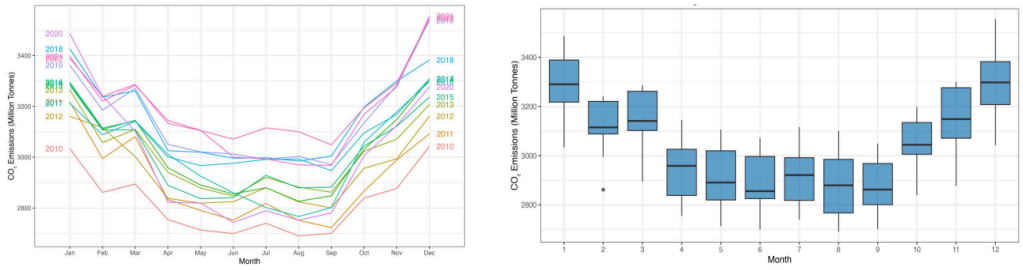


Figure 1. Global monthly CO_2 emissions from January 2010 to December 2022

DOI: 10.54254/2754-1169/2026.AB39173

The monthly series (as shown in Figure 1) ranges between roughly 2,700 and 3,550 Mt, combining a gentle upward trend with a highly regular annual cycle. The trend rises from about 2,780 Mt in 2010 to 3,140 Mt before 2020, dips to 2,960 Mt during the pandemic and recovers through 2021–2022.

In Figure 2, the seasonal sub-series and monthly boxplots show emissions peaking each December–January with Northern-Hemisphere heating and year-end industry, and bottoming in August–September; the median peak-to-trough difference exceeds 400 Mt.



(a) Seasonal global monthly CO_2 emission (b) Monthly distribution of global CO_2 emission

Figure 2. Annual seasonality of global CO_2 emissions

In Figure 3, the STL decomposition shows an almost unchanged twelve-month wave, while the remainder isolates the 2020 contraction. From Table 1, with the seasonal component accounting for 73.9% of short-term fluctuation, seasonality should be explicit.

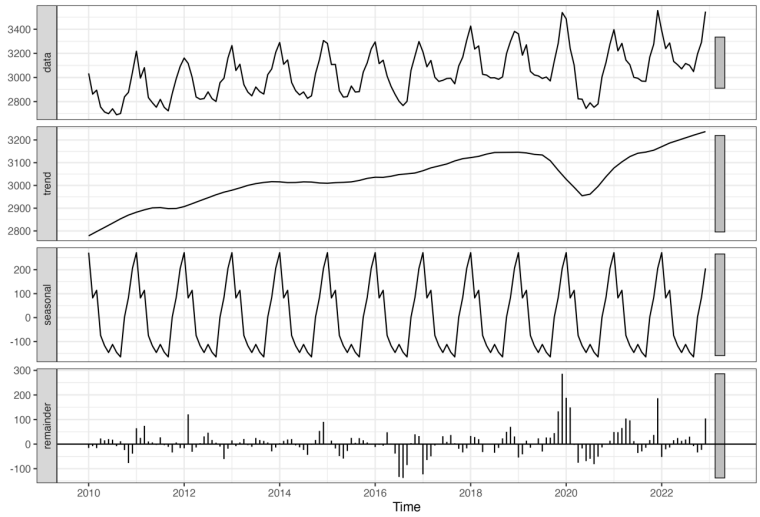


Figure 3. STL decomposition into observed data, trend, seasonal and remainder components

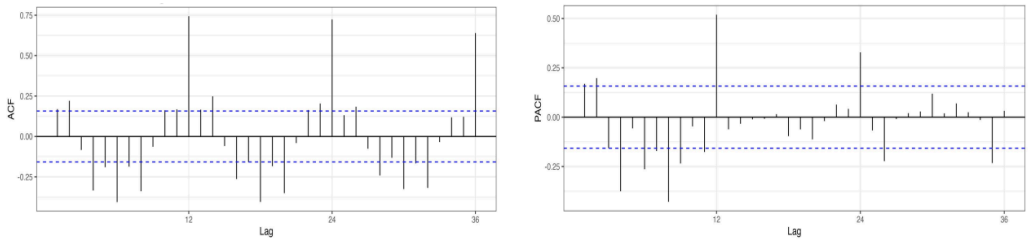
Table 1. Contribution of the seasonal component to short-term fluctuation

Indicator	Value
Seasonal contribution, sd(seasonal) / sd(series)	73.9%

DOI: 10.54254/2754-1169/2026.AB39173

4.2. Order identification and parameter estimates

The tests point to seasonal rather than regular differencing: the ADF test rejects a unit root ($p < 0.01$), so $d = 0$, while the differenced ACF/PACF (in Figure 4a and 4b) spike at lags 12, 24 and 36, indicating a twelve-month seasonal unit root removed by D=1. The exhaustive search selects ARIMA(1,0,0)(1,1,1) [12] with drift at the minimum AICc of 1,548.33. As shown in Table 2, the AR coefficient (0.82) shows strong persistence, the seasonal AR (−0.36) and MA (−0.61) encode annual reversal and smoothing, and the drift (2.35 Mt/month) quantifies modest growth.



(a) ACF of first differenced CO_2 series (b) PACF of first differenced CO_2 series

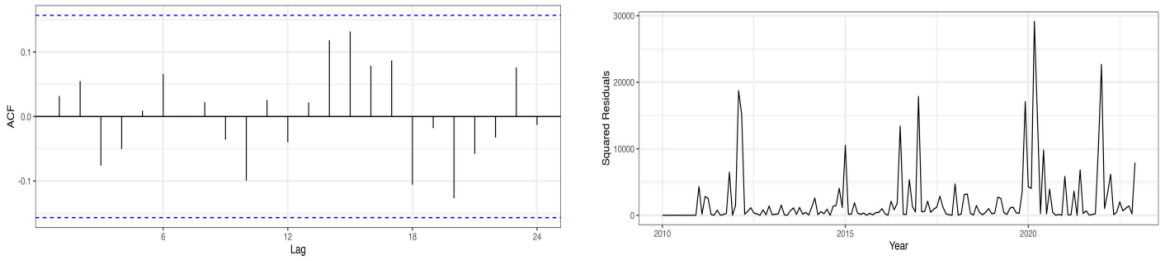
Figure 4. Correlograms of the first-differenced series

Table 2. Maximum-likelihood estimates of SARIMA(1,0,0)(1,1,1)12 with drift (full sample)

Parameter	Coefficient	Std. error
Non-seasonal autoregressive term, φ_1 (ar1)	0.8193	0.0508
Seasonal autoregressive term, Φ_1 (sar1)	−0.3617	0.1036
Seasonal moving-average term, Θ_1 (sma1)	−0.6120	0.1011
Drift, c (Mt per month)	2.3456	0.6144

4.3. Residual diagnostics

The mean-model residuals are serially uncorrelated: the Ljung–Box statistic at lag 12 gives $p = 0.9557$, and the residual ACF (as shown in Figure 5a) lies within the bands at virtually all lags (lag-one 0.03). The squared residuals (as shown in Figure 5b), however, cluster around 2020 and 2022, and the ARCH-LM test rejects constant variance ($p = 0.0164$), motivating the volatility stage.



(a) ACF of SARIMA residuals (b) Squared residuals

Figure 5. Residual diagnostics

DOI: 10.54254/2754-1169/2026.AB39173

4.4. Second-stage GARCH(1,1) volatility model

As reported in Table 3, a Gaussian GARCH(1,1) was fitted to the SARIMA residuals. All four parameters are significant at 5%: $\alpha_1 = 0.550$ means a 2020-type shock sharply raises next-month variance, and $\beta_1 = 0.344$ governs persistence; their sum ($0.894 < 1$) makes the variance stationary. Weighted Ljung–Box tests on standardised and squared residuals are insignificant (smallest p = 0.15), as are the ARCH test (p = 0.2747) and the Nyblom statistic (1.08), so the residuals are free of serial correlation and ARCH effects. Robust standard errors weaken the variance parameters, and a Pearson goodness-of-fit test rejects the Gaussian tail, favouring a fat-tailed Student-t GARCH for crisis periods.

Table 3. Gaussian GARCH(1,1) fitted to the SARIMA residuals (ordinary standard errors)

Parameter	Estimate	Std. error	p-value
Mean μ	7.8266	2.8594	0.0062
Constant ω	513.76	237.97	0.0309
ARCH α_1	0.5496	0.2167	0.0112
GARCH β_1	0.3439	0.1595	0.0311

4.5. Hold-out accuracy for 2022

As shown in Figure 6 and Table 4, MAPE rises to 2.55% and MASE to 0.97 from 1.01% and 0.37 in the 2010–2021 fit, yet Theil's U of 0.76 beats seasonal naïve extrapolation. The positive mean error (43.5 Mt) signals slight under-prediction as the 2020 rebound outran the model's path; such 2–3% errors compare favorably with recent work [9, 11].

Table 4. In-sample and 2022 out-of-sample forecast accuracy

Period	ME	RMSE	MAE	MPE	MAPE	MASE	ACF1	Theil's U
Training	1.40	44.63	30.86	0.03	1.01	0.37	0.06	—
Test (2022)	43.49	92.81	81.34	1.41	2.55	0.97	0.55	0.76

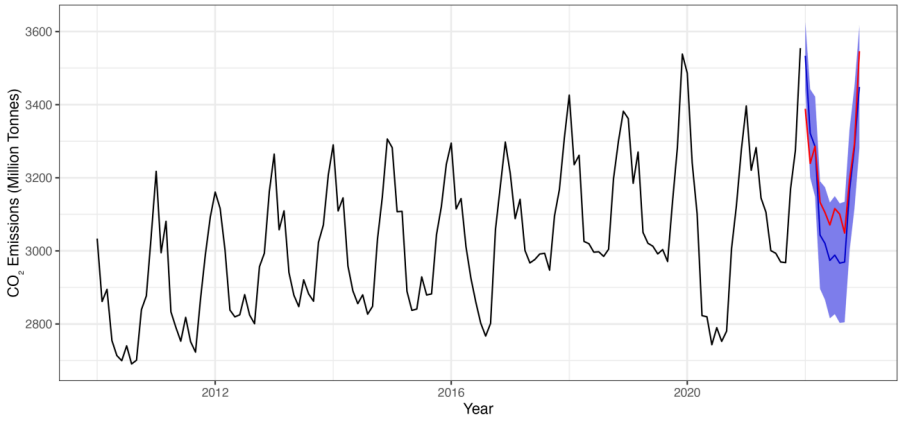


Figure 6. Twelve-month out-of-sample forecast for 2022 versus observed emissions

DOI: 10.54254/2754-1169/2026.AB39173

4.6. Twenty-four-month forecast and error analysis

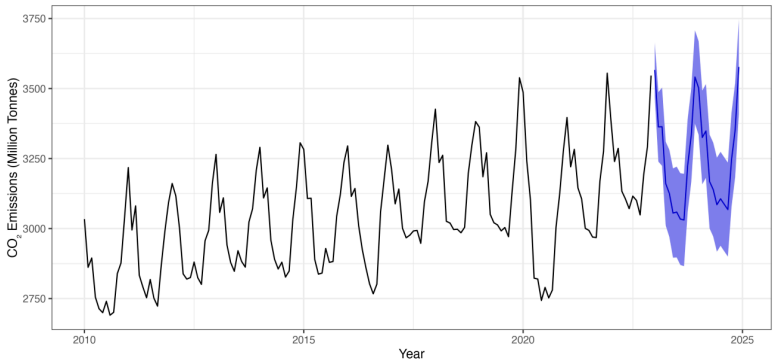


Figure 7. Twenty-four-month point forecast for 2023–2024 with 95% prediction intervals

The refitted model projects 2023–2024, retaining winter peaks and late-summer troughs. As shown in Figure 7, monthly values range from about 3,031 Mt (September 2023) to 3,577 Mt (December 2024), with the full table given in Table 5. Annual totals are 38.86 Gt in 2023 and 39.00 Gt in 2024, a rise of just 0.38%. The 95% intervals widen from ±96 to ±168 Mt by late 2024, and the near-plateau matches the Global Carbon Budget's 0.8% growth estimate for 2024 [5].

Table 5. Monthly point forecasts and 95% prediction intervals for 2023 and 2024

Month	2023 FC	Lo 95	Hi 95	2024 FC	Lo 95	Hi 95
January	3,566	3,470	3,662	3,502	3,335	3,669
February	3,363	3,239	3,487	3,325	3,158	3,492
March	3,364	3,224	3,503	3,348	3,181	3,516
April	3,161	3,011	3,310	3,168	3,001	3,335
May	3,125	2,970	3,281	3,139	2,972	3,307
June	3,055	2,896	3,215	3,085	2,918	3,253
July	3,059	2,897	3,221	3,106	2,939	3,274
August	3,034	2,870	3,198	3,087	2,919	3,254
September	3,031	2,866	3,196	3,068	2,900	3,235
October	3,224	3,059	3,390	3,245	3,078	3,413
November	3,334	3,168	3,501	3,352	3,185	3,520
December	3,541	3,375	3,708	3,577	3,409	3,745
Annual total	38,857	—	—	39,004	—	—

5. Policy recommendations

The monthly forecast baseline established in this study provides a reference for climate target tracking, abnormal emission identification and scenario comparison. Building on the empirical findings above, this section puts forward targeted mitigation recommendations from four dimensions.

DOI: 10.54254/2754-1169/2026.AB39173

5.1. Seasonal peak emission management

As seasonal variation accounts for nearly three quarters of short-term emission fluctuations, with the December–January peak over 400 Mt higher than the August–September trough, mitigation should be aligned with the annual cycle. Governments should prioritise winter peak demand reduction through building insulation retrofits, high-efficiency electric heating powered by low-carbon electricity, and demand-response mechanisms that flatten the seasonal load curve and reduce reliance on peaking fossil capacity.

5.2. Structural energy system transition

The projected 0.38% annual growth indicates a near-plateau rather than genuine decline. The pandemic demonstrated that emissions can drop by 6–7% in a single year, but such forced reductions reverse quickly once restrictions are lifted. Sustained emission cuts require replacing coal and gas with renewables and energy storage, electrifying industrial processes and building heating, and tightening mandatory energy efficiency standards.

5.3. Prioritisation of transport decarbonisation

As the sector most responsive to activity shocks and the largest single contributor to the 2020 emission drop, surface transport should be a policy priority. Measures include accelerating the rollout of electric vehicles, expanding public and active transport networks, and adopting travel-reduction policies such as remote work incentives and low-carbon urban planning.

5.4. Green fiscal policy and monthly monitoring

Fiscal policy should lock in long-term low-carbon investment, since carbon-intensive stimulus erases temporary emission gains whereas green recovery packages can bend the emission trajectory downward. Governments should institutionalise monthly emission monitoring and forecast-based early warning, so that deviations from the expected seasonal path trigger timely corrective policy action.

6. Conclusion

Using IEA–EDGAR global monthly fossil CO_2 emissions for 2010–2022, this study finds a mild upward trend, a sharp pandemic dip and rebound, and an annual cycle explaining 73.9% of short-term movement. The selected mean model is SARIMA(1,0,0)(1,1,1)12 with drift, with white-noise residuals (Ljung–Box $p = 0.96$), and a second-stage GARCH(1,1) (persistence 0.89) removes the ARCH effect. It achieves MAPE of 1.01% in sample and 2.55% for held-out 2022 and beats seasonal naïve forecasts (Theil's $U = 0.76$), projecting 38.86 Gt in 2023 and 39.00 Gt in 2024—a near-plateau insufficient for the 1.5 °C centigrade pathway, so structural, season- and sector-targeted mitigation is urgent.

Several limitations qualify the findings. First, the univariate mean model omits GDP, energy mix, fuel prices, policy and technology variables, so it implicitly assumes past patterns persist and cannot explain why emissions deviate. Second, infrequent structural breaks such as the 2020 pandemic are hard to estimate from only 156 observations, and the Gaussian GARCH exhibits fat-tailed mis-specification that may understate the depth of crisis-period shocks. Third, the monthly allocation relies on temporal profiles that are estimates rather than direct measurements, introducing

DOI: 10.54254/2754-1169/2026.AB39173

measurement error. Finally, the global aggregate masks large regional and sectoral differences, so the headline figure may conceal divergent trends in advanced and emerging economies, which limits its use for place-specific decisions.

These limitations point to four directions. Researchers can add exogenous variables in a SARIMAX framework to condition forecasts on output, prices and policy; replace the Gaussian variance equation with a Student-t or asymmetric GARCH for density forecasting; introduce explicit intervention terms that model crisis episodes; and compare forecast scenarios against nationally determined contributions and the 1.5 °C carbon budgets. Real-time evaluation against newly released monthly data would also establish whether the 2–3% hold-out errors remain stable outside a pandemic window, moving the model from short-term statistical tracking toward policy-attributable, probabilistic scenario analysis.

References

[1] United Nations Framework Convention on Climate Change. (2015). Paris Agreement. In *Report of the Conference of the Parties on its twenty-first session, held in Paris from 30 November to 13 December 2015—Addendum, part two: Action taken by the Conference of the Parties at its twenty-first session* (Decision 1/CP.21, FCCC/CP/2015/10/Add.1, pp. 1–27). https://unfccc.int/files/home/application/pdf/paris_agreement.pdf

[2] Intergovernmental Panel on Climate Change. (2021). *Climate change 2021: The physical science basis—Contribution of Working Group I to the Sixth Assessment Report of the Intergovernmental Panel on Climate Change* (V. Masson-Delmotte, P. Zhai, A. Pirani, S. L. Connors, C. Péan, S. Berger, N. Caud, Y. Chen, L. Goldfarb, & M. I. Gomis, Eds.). Cambridge University Press. https://doi.org/10.1017/9781009157896

[3] Le Quéré, C., Jackson, R. B., Jones, M. W., Smith, A. J. P., Abernethy, S., Andrew, R. M., De-Gol, A. J., Willis, D. R., Shan, Y., Canadell, J. G., Friedlingstein, P., Creutzig, F., & Peters, G. P. (2020). Temporary reduction in daily global CO_2 emissions during the COVID-19 forced confinement. *Nature Climate Change, 10*(7), 647–653. https://doi.org/10.1038/s41558-020-0797-x

[4] Liu, Z., Deng, Z., Zhu, B., Ciais, P., Davis, S. J., Tan, J., Andrew, R. M., et al. (2022). Global patterns of daily CO_2 emissions reductions in the first year of COVID-19. *Nature Geoscience, 15*(8), 615–620. https://doi.org/10.1038/s41561-022-00965-8

[5] Friedlingstein, P., O'Sullivan, M., Jones, M. W., Andrew, R. M., Hauck, J., Landschützer, P., Le Quéré, C., Li, H., Luijkx, I. T., Olsen, A., et al. (2025). Global carbon budget 2024. *Earth System Science Data, 17*(3), 965–1039. https://doi.org/10.5194/essd-17-965-2025

[6] Shan, Y., Ou, J., Wang, D., Zeng, Z., Zhang, S., Guan, D., & Hubacek, K. (2021). Impacts of COVID-19 and fiscal stimuli on global emissions and the Paris Agreement. *Nature Climate Change, 11*(3), 200–206. https://doi.org/10.1038/s41558-020-00977-5

[7] Box, G. E. P., Jenkins, G. M., Reinsel, G. C., & Ljung, G. M. (2015). *Time series analysis: Forecasting and control* (5th ed.). Wiley.

[8] Gogeri, I., Gouda, K. C., & Sumathy, T. (2024). Modeling and forecasting atmospheric carbon dioxide concentrations at Bengaluru city in India. *Stochastic Environmental Research and Risk Assessment, 38*(4), 1297–1312. https://doi.org/10.1007/s00477-023-02629-4

[9] Kumari, S., & Singh, S. K. (2023). Machine learning-based time series models for effective CO_2 emission prediction in India. *Environmental Science and Pollution Research, 30*(55), 116601–116616. https://doi.org/10.1007/s11356-022-21723-8

[10] Hu, J. B., Luo, Z. P., & Li, F. (2022). Forecasting China's carbon emission intensity toward the carbon-peak target: An analysis based on LSTM and ARIMA–BP models. *Finance and Economics, 2022*(2), 89–101.

[11] Zhang, J. F. (2024). Analysis of carbon emission forecasting in Gansu Province based on the ARIMA model. *Journal of Shanxi Datong University (Natural Science Edition), 40*(4), 31–36. https://doi.org/10.3969/j.issn.1674-0874.2024.04.008

[12] Crippa, M., Solazzo, E., Huang, G., Guizzardi, D., Koffi, E., Muntean, M., Schieberle, C., Friedrich, R., & Janssens-Maenhout, G. (2020). High resolution temporal profiles in the Emissions Database for Global Atmospheric Research. *Scientific Data, 7*, Article 121. https://doi.org/10.1038/s41597-020-0462-2

[13] Crippa, M., Guizzardi, D., Pagani, F., Banja, M., Muntean, M., et al. (2024). Insights into the spatial distribution of global, national, and subnational greenhouse gas emissions in the Emissions Database for Global Atmospheric

DOI: 10.54254/2754-1169/2026.AB39173

Research (EDGAR v8.0). *Earth System Science Data, 16*, 2811–2830. https://doi.org/10.5194/essd-16-2811-2024

[14] Cleveland, R. B., Cleveland, W. S., McRae, J. E., & Terpenning, I. (1990). STL: A seasonal-trend decomposition procedure based on loess. *Journal of Official Statistics, 6*(1), 3–73.

[15] Hyndman, R. J., & Koehler, A. B. (2006). Another look at measures of forecast accuracy. *International Journal of Forecasting, 22*(4), 679–688. https://doi.org/10.1016/j.ijforecast.2006.03.001